Region-based Abnormal Motion Detection in Video Surveillance

Jorge Henrique Busatto Casagrande[1] and Marcelo Ricardo Stemmer[2]

[1] *Núcleo de Telecomunicações, Instituto Federal de Santa Catarina, IFSC Campus São José,*
Rua José Lino Kretzer, 608, CEP 88103-310, São José, Santa Catarina, Brasil

[2] *Departamento de Automação e Sistemas, Universidade Federal de Santa Catarina, DAS/UFSC,*
CEP 88040-900 Caixa Postal 476, Florianópolis, Santa Catarina, Brasil

Keywords: Abnormal Motion Detection, Video Analysis, Automated Surveillance, Motion Analisys, Pattern Recognition.

Abstract: This article proposes a method to detect abnormal motion based on the subdivision of regions of interest in the scene. The method reduces the large amount of data generated in a tracking-based approach as well as the corresponding computational cost in training phase. The regions are spatially identified and contain data of transition vectors, resulting from the centroid tracking of multiple moving objects. On these data, we applied a one-class supervised training with one set of normal tracks on Gaussian mixtures to find relevant clusters, which discriminate the trajectory of objects. The lowest probability of transition vectors is used as the threshold to detect abnormal motions. The ROC (Receiver Operating Characteristic) curves are used to this task and also to determinate the efficiency of the model for each size increment of the region grid. The results show that there is a range of grid size values, which ensure a best margin of correct abnormal motions detection for each type of scenario, even with a significant reduction of data samples.

1 INTRODUCTION

In the last years, computer vision systems started to have an important contribution in capturing relevant information from scenarios and targets in video surveillance, since images taken by cameras have many similarities with the human vision. The information captured in this way help computer systems to make decisions about what they are "watching", similar to the human behavior. In that sense, one of the prominent applications of vision systems is the tracking of moving objects and inference about their behavior (Räty, 2010). The research in video surveillance around autonomous or automated systems seeks strategies that can improve results in pattern recognition and target behavior. The approaches generally prioritize ideas that require lower computational cost, in order to make feasible applications involving real-world scenarios and in different contexts (Sodemann et al., 2012). According these authors, effective approaches for motion analysis are pointing to spatio-temporal probability models. The inherent uncertainty of the observations in video scenes is a characteristic problem, which reinforces the use of probabilistic reasoning in the events modeling. Therefore, the most common machine modeling formalisms adopt Bayesian networks, HMM (Hidden Markov Models) and GMM (Gaussian Mixture Models) including their variations. For pattern recognition and training of these models, statistical learning methods such as the EM algorithm (Expectation Maximization) and kernel-based methods such as SVM (Support Vector Machines) are prevalent (Zeng and Chen, 2011), (Bishop, 2006).

1.1 Related Work

The authors who venture to design complete proposals, from the capture of video frames up to the behavior analysis of moving objects, need to determine constraints on their models in order to make feasible the computation of the heavy workload involved in every process (Berclaz et al., 2008), (Basharat et al., 2008), (Li et al., 2012), (Jiang et al., 2011). The works of these authors and (Ermis et al., 2008), (Kiryati et al., 2008), (Shi et al., 2010), (Hanapiah et al., 2010), (Feizi et al., 2012), (Haque and Murshed, 2012), (Cong et al., 2013) are generally focused on the search for better results on a set of standard video datasets created in their own trials or adopted from research groups around the world. Some approaches also deal with real world scenes, but are generally limited in flexibility in what concerns scenarios, targets, video length and reality. In addition, the use of heuris-

Busatto Casagrande J. and Ricardo Stemmer M..
Region-based Abnormal Motion Detection in Video Surveillance.
DOI: 10.5220/0004846607100717
In *Proceedings of the 3rd International Conference on Pattern Recognition Applications and Methods* (ICPRAM-2014), pages 710-717
ISBN: 978-989-758-018-5

tics is very common to simplify the modeling. Most of these papers are in another approach category into abnormal motion analysis: the motion-based. This category is attractive because it requires no preprocessing of video in opposite with tracking-based category which the robust tracking of multiple objects is still an open problem.

Previous research works have used the sub division of the region of interest in the scene in order to render processing more efficient, as well as methods to reduce dimensionality and computational cost. The so-called *curse of dimensionality* evaluated by (Bishop, 2006) is a recurring theme that requires a more sophisticated approach on *n*-dimensional data when *n* is greater than 3. The authors (Tziakos et al., 2010) used a grid of subregions as local abnormal motion detectors to test the effects of dimensionality reduction in unsupervised learning fashion. Authors such as (Elhoseiny et al., 2013) have consensus that it is necessary to use these techniques in combination with more robust and simple to implement classifiers. Otherwise it is impracticable to apply their ideas in the real world. We have adopted a scene modeling method similar to the one proposed in the framework implemented by (Li et al., 2012). However, the size of the grid regions in our case, isn't determined empirically. In the work of (Feizi et al., 2012), the number of pixels in the cluster size is conveniently determined by their method. Already the work of (Kwon et al., 2013) used the concept of entropy to adjust the size of the regions, which they named *cell* in order to tune the best data arrays that detect abnormal motions.

The authors (Basharat et al., 2008) developed a pixel-based method to identify abnormalities in both local and global motions[1] using GMM over a set of transition vectors stored at each pixel position. They noticed that the capture of transition vector data only from the centroid position of the objects made the motion modeling spatially sparse. This wasn't suitable for their learning model. Then, in each position occupied by moving objects, they copied the same vectors in all neighboring pixels up to the limit of the *bounding box* area of objects. The authors used a dataset with 1342 tracks that created a exponential density of samples. This helped to reduce the sources of errors in the learning model, but created computational constraints. The number of observable transitions defined as τ, had to be fixed at the limit of $\tau = 20$ to make the model computationally tractable.

1.2 Problem Description

This article focuses on the problem of the computational load required in pattern recognition of the tracking-based approaches, specifically when statistical models are adopted in training phases. In contrast to pixel-based solutions, this work presents a region-based method that aims to reduce the dimensionality of the involved data and maintains the inference quality of the abnormal motions detections.

Statistical models continue earning spaces to contribute to the solution of problems that emerge as challenges in the various processes of video analysis, in any category approach. The large amount of data required to be processed and the sophistication of the algorithms are presented as a barrier or even impediment for the computational treatment. (Shi et al., 2010) comment that real-time tracking-based category of all moving objects in complicated scenes is too difficult to achieve in real-world situations. We want to show that, adopting our method, this isn't a problem.

2 PROPOSED APPROACH

This paper intends to analyze changes in moving objects between regions larger than a single pixel of video resolution. As (Kwon et al., 2013), we understand that small displacements of the object centroid around a neighborhood of pixels has very little influence on the evaluation of the motion. Thus, ignoring the data portion representing these small movements, we will not significantly change the overall conclusion on the motion abnormality.

2.1 Assumptions

The analysis of abnormal motion is the last step of a tracking-based framework. Then, we concentrated only in this task isolating it from other processes. To take us faster the objectives, other assumptions and tools also were considered:

Motion, Scene and Learning Models. We adopted the similar models proposed by the authors (Basharat et al., 2008) applying however, the strategy of region-based analysis rather than pixel-based.

LOST Dataset. We used three sets containing 8 to 10 sequences of 30 minutes of the LOST Project videos (Longterm Observation of Scenes with Tracks Dataset) available by the authors (Abrams et al., 2012) at *http://lost.cse.wustl.edu*. The LOST dataset comprises several videos made from *streaming* of outdoor *webcams*, captured and organized by numbers

[1] According to the authors, local motions are those analyzed in the transition immediately after the current position of the moving object. The following transitions are associated with the global motion.

(1 to 25) in the same half hour every day at various locations around the world. The dataset contains metadata geolocation, object detection and tracking results. This dataset, among a number of surveyed such as (Oh et al., 2011) met the expectations of our work especially because it provides video annotations of objects tracking in different types of scenarios. We improve the tracking quality, selecting the best tracks and performing complementary annotations on video.

Off-line and Supervised Training. The GMM model was trained by the EM algorithm using the MATLAB functions *emgm.m* and *vbgm.m* (*http://www.mathworks.com/matlabcentral*). These functions implement the EM algorithms proposed by (Bishop, 2006) which it behaved better in accuracy and speed when compared to others proposed by (Figueiredo and Jain, 2002). These are alternatives to make the use of EM stable, bypassing the drawbacks when used in the standard form. The authors present algorithms that are able to select the number of components (clusters) automatically (unsupervised) and without the need for care in the initialization of finite mixture models belonging to multivariate data.

Homografy. Because the video sequences are captured from real video surveillance cameras outdoor, it becomes impractical to perform the *homography*, or perspective transformation through a camera calibration algorithm. Anyway, a real sense of depth and size or volume of objects in our analysis is irrelevant information since we are only interested in the centroid position in each transition track of the object;

Computational Cost Metric. The proposed method was implemented in MATLAB using a computer Pentium Intel®Core^{TM}i5 CPU M450@ 2.40GHzx4, 6GiB RAM and operating system Ubuntu 12.04LTS 64-bit. The measure of the computational cost, and rely on computational resources is sensitive to the structure of the algorithm adopted in the implementation of the method. Therefore, since there is a mathematical relationship between the computational cost with the number of samples involved in the process, we understand it is sufficient to use the total samples as a metric to quantify and compare the results. Unlike our approach, the time complexity is much more important to motion-based approaches because of the processing of each frame subregion is continuous. In our case, once the model is trained, the decisions are computed in $O(M)$ where M depends on τ and the number of moving objects in the frame. Otherwise, in motion-based, (Haque and Murshed, 2012) highlights that their complexity isn't higher than the pixel-based background subtraction process. (Shi et al., 2010) concludes with $\Theta(N^2 logN)$ for all their processes and N is the our p_u equivalent;

Annotated Dataset. We have classified the main types of objects and global motion on LOST dataset according Tables 1 and 2. These complementary annotations, turn the dataset an equivalent robust tracking step. Thus, we defined and left at disposition to use in simulations a 7-dimensional vector for each sample containing: 2D centroid coordinates in the frame resolution, the width and height of the *bounding box*, the *timestamp* of the transition, the class types of object and the global motion;

Table 1: Some object class types observed and annotated.

object type class (v)	description
1	1 person
4	2 persons group
7	bike
8	motorcycle
10	car/SUV
14	bus

Table 2: Object motion class types observed and annotated.

motion type class	description
0	Normal - usual path
1	Abnormal - unusual path
2	Abnormal - unusual local
3	Abnormal - unusual object

Dimensionality Reduction. We used for the purpose of training the model, only 3 of the 7 dimensions available in the dataset: the number of the region where the centroid is, the type of object and its *timestamp* in frame. The reduction of dimensions presented deviates our proposal from the curse of dimensionality problems. Obviously in a real application it would be necessary include in our proposal, both a robust tracking and a classifier that separates the object and motion types in multi-classes;

Abnormal Tracks. The video sequences of real scenes can not freely include abnormal tracks to form the test set to evaluate our method. However few inconsistencies contained in the LOST dataset, due to the simplicity of the tracking algorithm, are purposely held to be considered as motion abnormalities in the training phase. Examples of these anomalies are the tracking sudden changes that occur from occlusion between mobile objects. In this case, a track which starts associated with a car, can finish associated with a person from a occlusion region between them. This type of abnormality is labeled in video annotation with the number "1" from Table 2. In our implementation, we represented the motion and objects types by numbers placed above the *bounding box*. Figure 1 shows this detail.

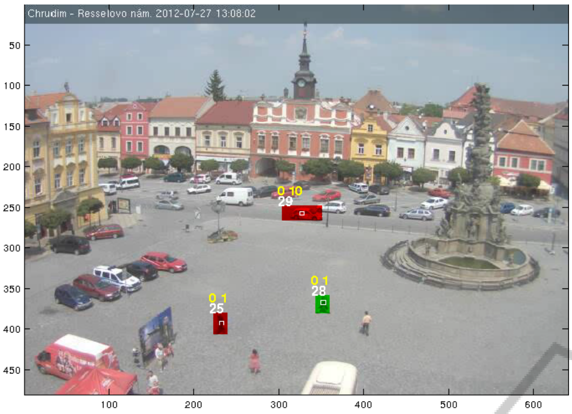

Figure 1: Sample of three objects in LOST video #1 using labeling according to Table 2 (above and left) and Table 1 (above and right). The white number represents the track.

2.2 Scene Modeling

Our idea is to cluster data in each region where the centroid of each object is observed. This region is a square area with side measuring p_u pixels which is defined here as **grid factor** and $p_u \in \mathbb{N}^*$. Then a fixed grid is defined with regions having a resolution equal to or less than the resolution of the video frame. Assuming the resolution frame $R \times C$ pixels, the regions $\{r_p\}_{p=1}^{g}$, are numbered sequentially from left to right and top to bottom turning the grid into a unidimensional vector of regions where $g = \lceil R/p_u \rceil . \lceil C/p_u \rceil$. In this respect, the two dimensions representing the position of the centroid of an object is reduced to a scalar that represents a position in the vector regions.

2.2.1 Grid Formation

The p index of the region r_p where the object centroid is located, can generically be determined by the expression $p = \lfloor (x_u - 1)/p_u \rfloor . \lceil C/p_u \rceil + \lceil y_u/p_u \rceil$, according to the current 2D centroid position (x_u, y_u) were $\{x_u\}_1^R$ and $\{y_u\}_1^C$. The region defined as r_1 of set $\{r_p\}_{p=1}^{g}$ is the first set of pixels from the top left of the frame. The region r_2 is immediately to the right of r_1 and so on up to the end of the columns or rows of the frame pixels. If C or R isn't a multiple of the size of p_u, the last regions on the rigth or bottom will have dimensions smaller than p_u but even so, they are labeled sequentially in the grid. Figure 2 illustrates an example of the grid regions r_p using a grid factor $p_u = 39$. The total area of the frame is transformed into a one-dimensional vector with $g = 221$ elements. For each frame, each object with respective 2D centroid coordinates, is associated with a single region even if the areas of the *bounding box* are overlapping the neighboring regions.

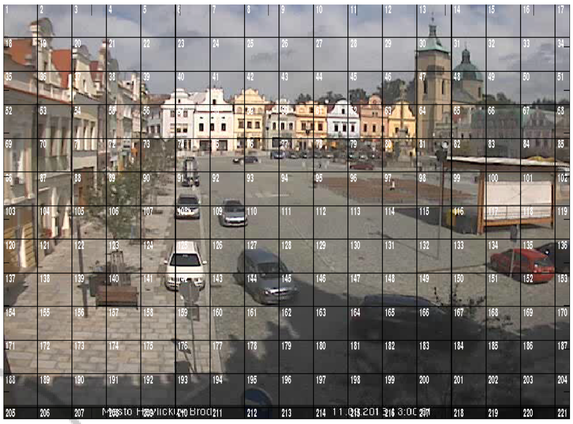

Figure 2: Labeling of grid formation over a generic frame of LOST video #17 with $R \times C = 480 \times 640$ pixels.

2.3 Motion Modeling

Each grid region is used as a reference to store all data vectors of a window of τ following object transitions. Obviously, the same region may belong to other object paths, and thus, accumulating an increasing amount of data. The transitions window defines how long the track of the object should be observed. The higher the value of τ, more specific becomes the analysis. The assumption to be a transition is considered when an object jumped to a different region in the next observation. Each track is observed within the limit of the window.

The annotated dataset offers a set of n tracks T for each video is represented as $\{T_i^k\}_{i=1}^{n}$ and $k \in \mathbb{N}^*$ is the set of frames k where the object is sampled. Each frame k has a well defined *timestamp* t in the video and $t \in \mathbb{R}^+$. Then T_i^k represents a set of m observations of the same object, $T_i^k = \{O_j^k\}_{j=1}^{m}$. Each observation is a set of transition vectors $O_j^k = \{\gamma_j^{j+a}\}_{a=1}^{\tau}$ were $\gamma_j^{j+a} = (r_p, v, t)^T$ is a vector transition sampled the trail and that contains the temporal continuous record t (*timestamp*) of object type v, in region r_p of the grid. Figure 3 shows these future transitions observation of any object in frame k in a sampling window up to τ. All transition vectors up to $\gamma_j^{j+\tau}$ are associated as samples at the region in the observation point O_j^k.

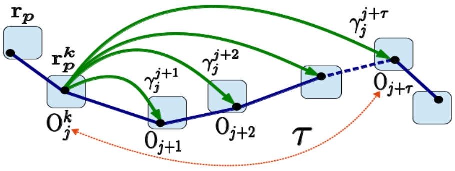

Figure 3: Detail of the motion model of a track T_i proposed by (Basharat et al., 2008) and adapted by us.

2.4 Learning Modeling

To build the database for training model, it is necessary the long-term observation of the scenes in order to obtain a sufficient samples of the objects types and their displacements. Therefore, we use three videos with different sizes according to Table 3. The characteristic of the scenarios and resolutions involved were purposely chosen. Video #1 has a more sparse number of tracks than the others. Video #14 has most of its tracks concentrated in specific regions of the scene. Figure 4 shows the detail of the distribution of tracks and samples of each video. The locations of pixels with more intense colors are those with the largest number of samples. The dispersion observed in samples videos #1 and #17 suggests that many areas may have insufficient data for training of the GMM.

Table 3: Data of the video datasets corresponding values achieved after training steps due to a factor grid $p_u = 1$.

LOST dataset	#1	#14	#17
resolution	480x640	240x320	480x640
hours	4	4	5
anormal tracks	37	32	116
normal tracks	1190	1755	2990
transitions	54661	58072	115688
samples	816018	777044	1646275

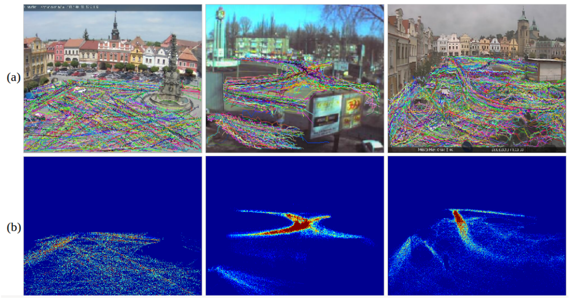

Figure 4: Scenarios samples used according to the LOST datasets. In (a) video #1, video #14 and video #17, in this order, In (b), the corresponding normalized distributions.

Any deviation of usual local or global motion, results in significant differences when calculating the probability and abnormalities are so identified. As an example, a person riding a motorcycle who moves on a trajectory and speed of usual pedestrians, should only be identified as an object with abnormal motion if it is on a sidewalk.

An iterative process conducted in off-line mode is done to find the value or range of values of p_u which leads to the best performance in the identification of abnormal motions. In the first step of training, all tracks annotated as abnormal, are excluded from the dataset. The sampling for each region is performed according motion model. Therefore, this method refers to a supervised learning since the training data consists of only one class normal events (Sodemann et al., 2012). In the second step, the dataset contain normal and abnormal events so that all tracks have annotations to be used as targets in lifting ROC curves. The found threshold represents the lowest probability of all transitions sampled in the scenario. Considering the dimensionality of data clusters equal 3, in summary, the probability is determined through equation (1), where η_p represents the samples quantity in each region r_p and $a = \{1, 2, ...\tau\}$.

$$P(\gamma_{j-a}|(\Sigma,\mu)_{r_p}) = \frac{1}{\sqrt{(2\pi)^3|\Sigma|\eta_p}} \exp^{-\frac{1}{2}(\Sigma-\mu)^T\Sigma^{-1}(\Sigma-\mu)} \qquad (1)$$

In each iteration we saved into vectors, the amount of samples used in the training steps and the threshold value associated with the best ROC curve efficiency. The value of p_u is incremented by one from the unitary value. After some experiments, our simulations are stopped for the value of $p_u = 30$. The limit of p_u increment and the metric ROC efficiency is discussed in section 3.

At the end of this process, one of the p_u values and respective best threshold ROC curve associated can be adopted for the monitored scenario. The known threshold is going to be used as a single-class classifier until the necessity of another round. Since both p_u and respective decision threshold values is chosen, any size or video sequence in the same video scenery which contains the annotations on its tracking, can be tested. One off-line round can be summarized in the following pseudo-code:

```
INITIALIZATION; pumax=30; tau=20; targets;
FOR pu=1 TO pumax
  \\ 1st Training Step with dataset one-class
  r(p)={}: p=1 TO ALL grid regions g;
  FOR all n tracks in each j transition
    JOIN in r(j+a),[r(j),v(j),t(a-j)],a=1:tau;
    FOR p=1 to g
      RUN EM over Gaussian Mixtures in r(p);
      SAVE learned parameters sigma_p,mu_p,k_p;
    END
  END
  \\ 2nd Training Step with full dataset
  FOR all n tracks in each j transition
    out_n = estimate min probability in r(j)|p
            from tau previous transitions;
  END
  RUN ROC curve from (out,targets)_n vector;
    threshold_n=ROC efficiency metric;
  PLOT samples_used and threshold_n by pu;
END
FIND best(pu,threshold) ranges among all plots;
END
```

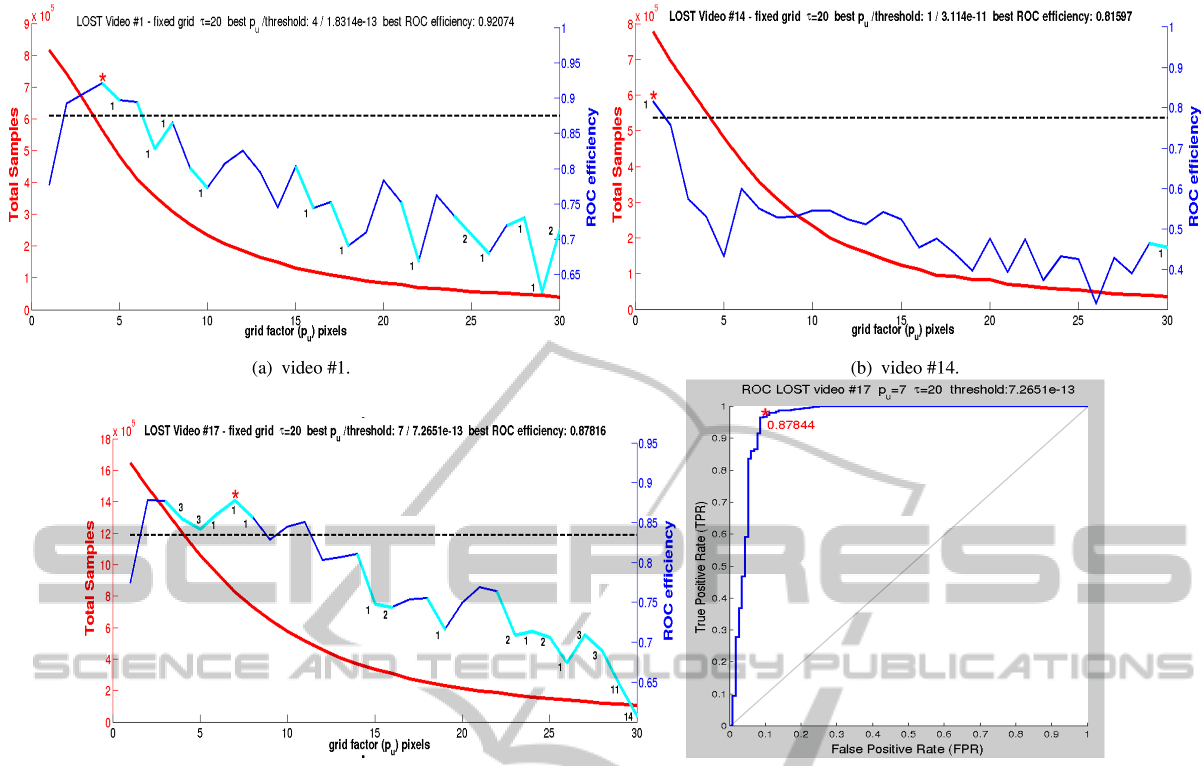

(a) video #1.

(b) video #14.

(c) video #17.

(d) Best ROC curve of video #17.

Figure 5: Effects of the increased grid factor over the amount of samples and the performance in abnormal motion detection.

On a test model, for each new position of each object in each frame and using equation (1), it is estimated the probability of that type of object to be at the current position and time, originating from each of the τ previous transitions (high order analysis). If any of the τ probabilities is less than the used threshold, then the object is identified as describing an unusual trajectory from that point until the end of its trajectory tracking in video. In our implementation, we highlight in red color the *bounding box* of the object that had its motion identified as abnormal.

3 RESULTS

In the context of this work, we have compiled the main data results through the curves shown in Figure 5. The curves show the relationship between the number of involved samples (red curves) and the ROC efficiency metric for each p_u value. For them, a transition windows $\tau = 20$ was adopted.

Since we are only interested in the highest hit rate of true positives (TPR) and the lowest hit rate of false positives (FPR), we adopted as reference metric the *ROC efficiency* through equation 2. (Powers, 2011) suggests a goodness performance measure for ($TPR - FPR$), called *informedness*. A number closer to 1, indicates better correct ratio for both abnormal and the normal tracks. The value of ε represents the number of lost tracks, which is explained hereafter.

$$ROCefficiency = (TPR - FPR).(1 - \frac{\varepsilon}{total\ tracks})^2 \quad (2)$$

As an example, the curve in Figure 5(c) shows that the best ROC efficiency value occurs when $p_u = 7$. The asterisk character presents the best outcome of the equation 2. Figure 5(d) shows the detail of best ROC curve and corresponding threshold value.

The numbers alongside different color segments plotted in the ROC efficiency curve, represent the amount of tracks that have been lost for two reasons: (i) the number of samples in all object transition regions wasn't enough for the convergence of the GMM training algorithm (usually the clusters require at least 30 samples) and (ii) lack of transitions between regions. In our tests, the hypothesis (i) was most representative. These losses are well demonstrated in videos #1 and #17 due to fact that they have a sample dispersion in many regions of interest, as shown in Figure 4 (b). The hypothesis (ii) becomes relevant for larger p_u values. Higher values of p_u decreases the transitions amounts. These larger regions can contain most or all samples of a shorter track. This was the reason why we adopt the limit $p_u = 30$, because from that value on, the loss of tracks get larger. When tracks are lost, they affect TPR and FPR ratios and become unequal in results comparison. To avoid this negative influence, we apply a penalty factor according to equation (2) which takes into consideration the loss of ε tracks in relation to the total tracks.

We consider an optimal range of grid factors p_u for each LOST video. This range must have a minimum track loss and must not be less than the value when $p_u = 1$. The boundary of this range in Figure 5 is represented by the horizontal dashed line. It is also clear that in all tested videos there is a common performance improvement when $1 \lesssim p_u \lesssim 10$. In this range, the number of samples decreases up to $\sim$60% if compared with equivalent pixel-based models (when $p_u = 1$). This is the case of video #17 were the number of samples starts in $\sim$1.64 milion when $p_u = 1$ and decreases to 648,483 when $p_u = 9$.

If we extend the comparison with the previous approach presented by (Basharat et al., 2008), the difference is huge due to the motion model these authors makes sample copies in all pixels of *bounding box* boundary. In a simulation using the dataset available by the authors, with video resolution 240x320 pixels and $\sim$3 hours length, we observed more than 250 million samples and the ROC curve with much lower performance than we present in Figure 5(d).

The training time was dependent on the video according to the samples concentration per region. So, considering the best value of p_u, all videos had their training time much lower than total time of the videos.

The input vector for the space-time motion model is reduced to a 3-dimensional space with (r_p, v, t). The distribution of the data vectors in hyperplanes tends to be sparse. This harms the accuracy and convergence of the GMM models. Otherwise, too many samples, or oversampling form a lot of less representative clusters which require more unnecessary computational effort. In videos #1 and #17 it is notable the fast efficiency increasing from $p_u = 1$. This is an expected effect because the increasing of regions area, samples will be adding in these regions and help to ensure or to improve the clusters during GMM training. This behavior isn't observed with video #14 due to the higher concentration of samples in a small area in the center of the video even when $p_u = 1$ (see detail in Figure 4 (b)). When $p_u > 1$ an oversampling occurs and this saturation has not produced good results in the GMM training. The behavior leads to the conclusion that region-based models do not require many samples, however they need to be better distributed.

4 FURTHER WORKS

The method has shown insensitivity to scene context and low dependency on the robustness of the tracking algorithm. The uniform behavior of the performance curves revels these tendency, since they deal with different resolutions, areas of interest, object's *bounding box* fidelity and their tracking, number of track transitions, number of tracks and video length. In this aspect, the LOST project opens opportunities for research in scene analysis involving long-term surveillance in outdoor environments. We intend to use it also for future studies, including the application of the same method presented here, but using others statistical models such as HMM.

We observe that the p_u range values which leads to the best performance of the method, tend to match with the smallest object size tracked (high or width). These information did not explicitly participate in the training. Currently, we are engaged in evidence and theoretical explanation of this trend.

We intend to continue the study of this approach using a mobile grid rather than a fixed one, as well as using algorithms like superpixel segmentation.

Alternatively, since the computational effort is reduced due to the lower amount of samples, it is possible to keep a training window in on-line mode. Simply replacing old samples and repeating the GMM model training only for updated regions.

5 CONCLUSIONS

We present a new method for abnormal motion detection in real video surveillance scenes. We complemented with video annotations the preexisting tracks of the LOST dataset. The proposed region-based method supported by ROC curves, used scene, motion and learning models focused on dimensionality reduction to decrease the computational effort without sacrificing performance in detecting abnormalities. Our method avoids the excessive data and sophisticated algorithms used in many pixel-based approaches. In addition, appearance models of objects did not need to be defined, like most of the region-based strategies.

Our results show that the method is useful and also shown good behavior for different scenarios, contexts, quantity and quality of samples. They have demonstrated that there is a range of grid factor values that maintain the efficiency in motion analysis, even with a significant reduction in the number of samples used to train a statistical model such as the GMM.

REFERENCES

Abrams, A., Tucek, J., Little, J., Jacobs, N., and Pless, R. (2012). LOST: Longterm Observation of Scenes (with Tracks). In *Applications of Computer Vision (WACV), 2012 IEEE Workshop on*, pages 297–304.

Basharat, A., Gritai, A., and Shah, M. (2008). Learning object motion patterns for anomaly detection and improved object detection. In *Computer Vision and Pattern Recognition, 2008. CVPR 2008. IEEE Conference on*, pages 1–8.

Berclaz, J., Fleuret, F., and Fua, P. (2008). Multi-camera Tracking and Atypical Motion Detection with Behavioral Maps. In *ECCV (3)*, pages 112–125.

Bishop, C. M. (2006). *Pattern Recognition and Machine Learning*. Springer, New York.

Cong, Y., Yuan, J., and Tang, Y. (2013). Video Anomaly Search in Crowded Scenes via Spatio-Temporal Motion Context. *IEEE Transactions on Information Forensics and Security*, 8(10):1590–1599.

Elhoseiny, M., Bakry, A., and Elgammal, A. (2013). Multi-Class Object Classification in Video Surveillance Systems Experimental Study. In *CVPR'13*, pages 788–793.

Ermis, E. B., Saligrama, V., Jodoin, P.-M., and Konrad, J. (2008). Motion segmentation and abnormal behavior detection via behavior clustering. In *ICIP*, pages 769–772. IEEE.

Feizi, A., Aghagolzadeh, A., and Seyedarabi, H. (2012). Behavior recognition and anomaly behavior detection using clustering. In *Telecommunications (IST), 2012 Sixth International Symposium on*, pages 892–896.

Figueiredo, M. A. T. and Jain, A. (2002). Unsupervised learning of finite mixture models. *Pattern Analysis and Machine Intelligence, IEEE Transactions on*, 24(3):381–396.

Hanapiah, F., Al-Obaidi, A., and Chan, C. S. (2010). Anomalous trajectory detection using the fusion of fuzzy rule and local regression analysis. In *Information Sciences Signal Processing and their Applications (ISSPA), 2010 10th International Conference on*, pages 165–168.

Haque, M. and Murshed, M. (2012). Abnormal Event Detection in Unseen Scenarios. In *Multimedia and Expo Workshops (ICMEW), 2012 IEEE International Conference on*, pages 378–383.

Jiang, F., Yuan, J., Tsaftaris, S. A., and Katsaggelos, A. K. (2011). Anomalous video event detection using spatiotemporal context. *Computer Vision and Image Understanding*, 115(3):323–333.

Kiryati, N., Riklin-Raviv, T., Ivanchenko, Y., and Rochel, S. (2008). Real-time abnormal motion detection in surveillance video. In *ICPR*, pages 1–4. IEEE.

Kwon, E., Noh, S., Jeon, M., and Shim, D. (2013). Scene Modeling-Based Anomaly Detection for Intelligent Transport System. In *Intelligent Systems Modelling Simulation (ISMS), 2013 4th International Conference on*, pages 252–257.

Li, H., Achim, A., and Bull, D. (2012). Unsupervised video anomaly detection using feature clustering. *Signal Processing, IET*, 6(5):521–533.

Oh, S., Hoogs, A., Perera, A. G. A., Cuntoor, N. P., Chen, C.-C., Lee, J. T., Mukherjee, S., Aggarwal, J. K., Lee, H., Davis, L. S., Swears, E., Wang, X., Ji, Q., Reddy, K. K., Shah, M., Vondrick, C., Pirsiavash, H., Ramanan, D., Yuen, J., Torralba, A., Song, B., Fong, A., Chowdhury, A. K. R., and Desai, M. (2011). AVSS 2011 demo session: A large-scale benchmark dataset for event recognition in surveillance video. In *AVSS*, pages 527–528. IEEE Computer Society.

Powers, D. M. W. (2011). Evaluation: From Precision, Recall and F-Factor to ROC: Informedness, Markedness & Correlation. *Journal of Machine Learning Technologies*, 2(Issue 1):37–63.

Räty, T. (2010). Survey on Contemporary Remote Surveillance Systems for Public Safety. *Systems, Man, and Cybernetics, Part C: Applications and Reviews, IEEE Transactions on*, 40(5):493–515.

Shi, Y., 0001, Y. G., and Wang, R. (2010). Real-Time Abnormal Event Detection in Complicated Scenes. In *ICPR*, pages 3653–3656. IEEE.

Sodemann, A. A., Ross, M. P., and Borghetti, B. J. (2012). A Review of Anomaly Detection in Automated Surveillance. *IEEE Transactions on Systems, Man, and Cybernetics, Part C*, 42(6):1257–1272.

Tziakos, I., Cavallaro, A., and Xu, L.-Q. (2010). Local Abnormality Detection in Video Using Subspace Learning. In *Advanced Video and Signal Based Surveillance (AVSS), 2010 Seventh IEEE International Conference on*, pages 519–525.

Zeng, S. and Chen, Y. (2011). Online-learned classifiers for robust multitarget tracking. In *Neural Networks (IJCNN), The 2011 International Joint Conference on*, pages 1275–1280.